Ann. For. Sci. 59 (2002) 141–154

DOI: 10.1051/forest:2002001

Original article

A flexible radial increment taper equation derived from a process-based carbon partitioning model

Christine Deleuze [a]* and François Houllier [b]

[a] Équipe ENGREF/INRA Dynamique des Systèmes Forestiers, ENGREF, 14 rue Girardet, 54042 Nancy Cedex, France
[b] UMR CIRAD-CNRS-INRA-Université Montpellier II Botanique et Bioinformatique de l'Architecture des Plantes (AMAP), CIRAD, TA40/PS2, Boulevard de la Lironde, 34398 Montpellier Cedex 5, France

(Received 29 November 2000; accepted 8 March 2001)

Abstract – Carbon allocation to the cambium along the stem is represented by a reaction-diffusion model along a continuous sink. Vertical variations of stem area increment along the stem are then theoretically connected to partitioning coefficients between tree compartments, at different spatial scales. This model is very sensitive to environmental growth conditions, and demonstrates the importance of topology and geometry in models of secondary tree growth. An analytical resolution is proposed to describe the vertical profile of stem area increment between crown basis and soil level. An empirical parametric equation is derived from this theoretical model. The 3 parameters of this equation are related to the internal and environmental conditions of the tree. These parameters can be used as indicators in order to study the variability of stem taper. This equation is separately fitted on data from two experiments, with different silviculture and site quality, for Picea abies of different ages. Variation in the parameters is discussed according to growth conditions. This equation is further integrated in order to predict stem volume increment. Finally, some simple characteristic heights are derived from this function as indicators of functional crown basis. These heights are systematically calculated to predict crown recession. They are finally compared to heights measured during field work.

allocation / cambium / carbon / functional crown height / reaction-diffusion

Résumé – Une fonction d'accroissement ligneux le long de la tige, déduite d'un modèle à base physiologique d'allocation du carbone. La distribution du carbone le long du tronc est décrite par un modèle de réaction-diffusion le long d'un puits continu de carbone : le cambium. L'accroissement ligneux le long de la tige se déduit donc d'un modèle d'allocation de carbone dans l'arbre, à une échelle fine. Ce modèle permet de prendre en compte l'effet des variations environnementales sur les profils de tige. Il montre le lien étroit entre topologie et physiologie pour la croissance secondaire. Une solution analytique de ce modèle permet de décrire l'accroissement ligneux en dessous de la base de houppier. À partir de ce modèle théorique, nous proposons une fonction empirique pour décrire l'accroissement ligneux tout le long de la tige. Cette fonction comporte 3 paramètres dont les variations peuvent être reliées aux conditions environnementales. Cette fonction est ajustée à des données d'analyses de tiges d'épicéas avec des âges, des sylvicultures et des fertilités différents. Les paramètres sont discutés selon les conditions de croissance. Une intégration de cette fonction permet un calcul analytique de la production en volume. Enfin la fonction est dérivée pour obtenir des hauteurs caractéristiques, indicatrices de la base du houppier fonctionnel. Ces hauteurs sont calculées pour décrire rétrospectivement les remontées du houppier et sont comparées aux mesures externes de houppier, l'année d'abattage.

allocation / cambium / carbone / base de houppier fonctionnel / réaction-diffusion

* Correspondence and reprints
Tel. (33) 3 80 36 36 20; Fax (33) 3 80 36 36 44; e-mail: nordest@afocel.fr
Present address: AFOCEL Nord-Est, Route de Bonnencontre. 21170 Charrey-sur-Saône, France

1. INTRODUCTION

Traditional stem taper equations focus on the cumulated output of tree growth. However the geometrical distribution of the radial increments is of prime importance for timber quality: according to species, wood properties can indeed be predicted from ring age and/or ring width [17]. On the other hand, stem analysis techniques are often used by forest biometricians in order to calibrate growth and yield models: these techniques result in sets of geometrical stem data (i.e., heights and radii). Some growth models have explicitly focused on such a geometrical description [26, 40]. In our laboratory, such a model was built for Norway spruce [17].

Deleuze and Houllier [6] presented a process-based version of this model. As an output they obtained the simulated inner ring structure of the stem. This model was based on the carbon balance of the tree, and wood increment was distributed along the stem by an allometrical relationship between stem area increment at any point along the stem and foliage biomass above this point (the so-called Pressler rule (1865) in [1]): "The area increment on any part of the stem is proportional to the foliage capacity in the upper part of the tree, and therefore is nearly equal in all parts of the stem, which are free from branches".

In fact, the empirical Pressler rule is not valid when environmental conditions vary [9, 21, 32]: (i) open-grown trees and dominant trees growing in good conditions have a steeper taper and a bigger buttress; (ii) suppressed trees have a thinner or no increment at the base of the stem [20, 27]; (iii) Pressler rule never describes the buttress [31]. Stem profile is indeed affected by total carbon production, therefore by social position of the tree. It is also affected by fertilization [10, 18, 37].

Pressler rule exactly corresponds to the hypothesis of a uniform carbon allocation along the stem. Divergence from this rule may be seen as a vertical variation of partitioning coefficients related to environmental changes. These empirical observations clearly indicate that Pressler rule is too rigid and that we need more flexible models, which can be linked with environmental parameters.

The aim of this paper is to propose new flexible equations of stem area increment along the stem. These equations are heuristically derived from a process-based model, in which the portion of the stem located between foliage and soil level is considered as a continuous carbon sink. According to this description, the vertical partitioning of carbon is represented by a one-dimensional reaction-diffusion model, where the diffusion term stands for carbohydrate translocation along the stem [7], while the reaction term stands for the utilization of carbohydrates by the cambium for its growth. Reaction-diffusion models have already been used in mathematical ecology [12, 28, 30] and in forest modeling [3, 13–15]. These models focus on population dynamics, while ours focuses on carbon dynamics and fixation along the stem.

This process-based model yields a system of partial derivatives equations. In this paper, we analytically solve this differential system under simple assumptions, and we derive explicit solutions which generate a simple and flexible function that describes the vertical profile of annual stem area increment along the stem. This equation has only three parameters and can be interpreted according to tree physiological status.

Picea abies stem analysis data are used to fit this model, and the value of model parameters is discussed according to the prevailing site and silvicultural conditions. This function is further used to estimate stem volume increment. Three characteristic heights are also derived from this function. They drive us to a better definition of the functional crown. These theoretical heights are compared to observed values: height to the first living branch, height to the first living whorl, and height to the first contacts with neighbor crowns.

2. DATA

2.1. Moncel-sur-Seille site

In 1991, 53-year-old trees were felled and measured in 4 pure even-aged stands of *Picea abies* located on a flat area at Moncel-sur-Seille, near Nancy (northeastern France). These stands corresponded to 2 site quality levels by 2 thinning intensities: ("s1") high productivity and high thinning intensity, ("s2") high productivity and low thinning intensity, ("s3") low productivity and high thinning intensity, ("s4") low productivity and low thinning intensity. In each stand, 6 trees were selected: 2 dominant, 2 codominant and 2 suppressed [16].

2.2. Amance site

The second site was located at Amance, near Nancy. The pure even-aged experimental stand ("s5") of *Picea abies* (L.) Karst. was planted in 1970 on a flat area with a

relatively good site index [4]. Two provenances were mixed (Istebna, Poland, and Morzine, Northern Alps, France) along a 50 m East-West gradient. Stand density varied continuously along a linear 75 m North-South gradient from open growth to 10 000 stems/ha. The trial had been slightly thinned in 1983 [8]. In January 1993, 4 dominant trees were selected at random in the 100% Istebna part of the plot at different densities: tree "a1" was an open-grown tree, while tree "a2" and tree "a117" were located in medium-density part of the stand (1 000–4 000 stems/ha) and tree "a134" was situated in the densest part of the stand [5].

2.3. Measurements

For each tree, we measured: the total height (H), the diameter at breast height (DBH), the height to the lowest living branch (H_{fb}), the height to the lowest living whorl (with at least three quarters of living branches: H_{fw}), and the height of the first whorl free of any contact with neighbor trees (H_{fc}). One of the objectives of the paper was to get a better understanding of the functional meaning of these alternative definitions of crown basis.

From the scars located at the top of each stem growth unit [2], height growth was described throughout the life of the tree. Disks were then cut from each tree in order to obtain a description of annual increment along the stem: 11 or 12 disks for trees from Moncel-sur-Seille and one disk per growth unit for trees from Amance.

3. THE REACTION-DIFFUSION MODEL

3.1. Structure of the model

The model was initially built for conifers, and was derived by Deleuze and Houllier [7] from the continuous formulation of carbon transport resistance in Thornley's model [38, 39]. In fact, it combines two processes that take place along the stem: a carbon diffusion process, and a carbon consumption process, i.e., secondary growth is viewed as a *continuous sink*. In its original version, the model is restricted to the portion of the stem located between crown basis and roots.

The height to the base of the functional part of the crown is noted H_c: according to the definition of the "functional crown", H_c may thus be H, H_{fb}, H_{fw} or H_{fc}. We consider the portion of the stem situated below H_c, and note x the vertical abscissa along the stem measured downwards from crown basis: $x = 0$ at crown basis, and $x = H_c$ at soil level.

At time t, stem radius and stem section are respectively noted $R(x,t)$ and $G(x,t) = \pi R^2(x,t)$, while $P(x,t)$ is the concentration of photosynthates in the phloem. Over a time step Δt (say, 1 year), stem radial and stem section increment are respectively defined as:

$$\begin{cases} \Delta R(x,t) = \int_0^{\Delta t} \dfrac{\partial R(x,t)}{\partial t}\, d\tau \\ \Delta G(x,t) = 2\pi \int_0^{\Delta t} R(x,t)\, \dfrac{\partial R(x,t)}{\partial t}\, d\tau. \end{cases} \quad (1)$$

The reaction-diffusion model is a system of two coupled partial derivatives equations in P and R. The temporal rate of change in the concentration of photosynthate ($\frac{\partial P(x,t)}{\partial t}$, kg C m^{-3} yr^{-1}) is the balance between a diffusion ($\frac{\partial^2 P(x,t)}{r \partial x^2}$) with a resistance r (yr m^{-2}), and a consumption of carbon for stem growth ($2\pi a R \frac{P(x,t)}{S}$) (see [7] for more details and for numerical solutions):

$$\begin{cases} \dfrac{\partial P(x,t)}{\partial t} = \dfrac{\partial^2 P(x,t)}{r \partial x^2} - 2\pi a R \dfrac{P(x,t)}{S} \\ \dfrac{\partial R(x,t)}{\partial t} = a \dfrac{P(x,t)}{\rho} \end{cases} \quad (2)$$

where S, r, a and ρ are parameters (see *table I*). S is the cross sectional area of the phloem (m^2), a is the stem growth rate or carbon consumption rate (m yr^{-1}), and ρ is the dry weight of carbon per unit fresh wood volume (kg C yr^{-1}). This system is completed by limit conditions (see below).

3.2. Analytical resolution of the model

First, we look for simple analytical solutions of equation (2). R is the stem radius, so that this variable cannot be stationary. However, we can look for solutions that are stationary for P, i.e. $P(x,t) = P(x)$. For such solutions, $\frac{\partial R(x,t)}{\partial t} = \alpha(x)$ and $R(x,t) = \alpha(x)t + \beta(x)$, where $\alpha(x)$ and $\beta(x)$ are constant and only depend on x. System (2) then becomes:

$$\frac{\partial^2 P(x)}{r \partial x^2} = 2\pi a(\alpha(x)t + \beta(x))\frac{P(x)}{S}. \quad (3)$$

Table I. Parameters and variables in the reaction-diffusion model.

Name	Meaning	Unit
x	Downward distance from crown basis	m
t	Time	year (yr)
$P(x,t)$	Photosynthates concentration in the phloem	kg C m^{-3}
$R(x,t)$	Stem radius	m
r	Resistance along the phloem	yr m^{-2}
S	Phloem cross sectional area	m^2
a	Stem growth rate	m yr^{-1}
ρ	Dry weight of carbon per unit of fresh wood volume	kg C m^{-3}
ΔC_r	Carbon allocation to the roots	kg C yr^{-1}
ΔC_s	Carbon allocation to the stem	kg C yr^{-1}
R_0	Initial stem radius for a cylinder	m
ε	Slope of the conical shape of the stem	unitless
H_c	Stem length (between "crown basis" and soil level or between tree tip and soil level)	m
P_f	Carbon foliage concentration	kg C m^{-3}
P_r	Carbon roots concentration	kg C m^{-3}
F_f	Carbon flow from foliage	kg C m^{-3} yr
F_r	Carbon flow to the roots	kg C m^{-3} yr
$\Delta G(x,t)$	Annual stem area increment	m^2 yr^{-1}
H_{fb}	Height to the lowest living branch	m
H_{fw}	Height to the lowest living whorl	m
H_{fc}	Height of the first whorl free of any contact with neighbor trees	m

This equation does not depend on t, so that $\alpha(x) = 0$, $\frac{\partial R(x,t)}{\partial t} = 0$ and $P(x,t) = 0$: stationary solutions for P are thus trivial for R.

Therefore, there is no general stationary solution that is non trivial for system (2). However, we can look for analytical solutions under the following approximation: if radial increment is assumed to be very small during the course, we can neglect the evolution of R: $R(x,t) \approx R(x)$. In that case, the resolution of equation (1) depends on the profile of $R(x)$. In this paper, we consider two simple cases for the initial stem profile: a cylinder or a cone.

3.2.1. Approximate steady-state solutions for an initial cylindrical stem

Under this initial condition and assuming that radial increment can be neglected: $R(x,0) = R_0$. Looking for simple stationary solutions for P (see Appendix 1 for a non-steady state solution), we get an ordinary second order differential equation in P:

$$\frac{\partial P(x,t)}{\partial t} = 0 = \frac{\partial^2 P(x,t)}{r \partial x^2} - a' P(x,t) \qquad (4)$$

where $a' = 2\pi a R_0/S$. General solutions of this equation are linear combinations of exponential functions [11]:

$$P(x,t) = P(x) = A\exp(-zx) + B\exp(zx), \qquad (5)$$

where $z = \sqrt{a'r}$.

The final solution depends on conditions at limits (i.e., foliage and roots).

In this case, the instantaneous radial increment, which is proportional to photosynthates concentration, does not depend on t, but only on x: $\frac{\partial R(x,t)}{\partial t} = a \frac{P(x)}{\rho}$. It is therefore

possible to simply compute the stem area increment $\Delta G(x)$ over Δt: $\Delta G(x)$ is indeed proportional to $P(x)$:

$$\Delta G(x) = 2\pi R_0 \int_0^{\Delta t} a \frac{P(x)}{\rho} \mathrm{d}\tau = \frac{2\pi R_0 a}{\rho} P(x)\Delta t. \quad (6)$$

It is thus possible to analytically compute the radius of the stem after Δt, as well as the stem: root allocation ratio of photosynthates ($\Delta C_s/\Delta C_r$) over the same period:

$$R(x,t) = R_0 + \int_0^{\Delta t} \frac{a}{\rho} P(x,\tau)\,\mathrm{d}\tau = R_0 + \frac{a}{\rho} P(x)\Delta t. \quad (7)$$

$$\Delta C_s(t) / \Delta C_r(t) = \frac{\int_{\tau=0}^{\Delta t} \int_{x=0}^{H_c} P(x,\tau)\mathrm{d}x\mathrm{d}\tau}{\int_{\tau=0}^{\Delta t} \int_{x=H_c}^{\infty} P(x,\tau)\mathrm{d}x\mathrm{d}\tau} = \frac{\int_{x=0}^{H_c} P(x)\mathrm{d}x}{\int_{x=H_c}^{\infty} P(x)\mathrm{d}x}. \quad (8)$$

3.2.2. Approximate steady-state solutions for an initial conical stem

Under this initial condition and assuming that radial increment can be neglected: $R(x,t_0) = R_0 + \varepsilon x$. We again look also for stationary solutions in P (to our knowledge, the system cannot be solved in non-steady state). The system (2) becomes:

$$\frac{\partial P(x,t)}{\partial t} = \frac{\partial^2 P(x,t)}{r\partial x^2} - 2\pi a(R_0 + \varepsilon x)\frac{P(x,t)}{S}. \quad (9)$$

With a translation of R_0/ε for x, this system is equivalent to:

$$\frac{\partial^2 P(x)}{r\partial x^2} - 2\pi a \varepsilon x \frac{P(x)}{S} = 0. \quad (10)$$

$P(x)$ is a combination of two independent solutions P_1 and P_2, which are themselves combinations of the hyperbolic Bessel functions: I^+ and I^- (see Appendix 2). As in equation (6), stem area increment can then be easily computed:

$$\Delta G(x) = \frac{2\pi(R_0 + \varepsilon x)a}{\rho} P(x)\Delta t. \quad (11)$$

3.3. General shape of the solutions

In both above studied cases, the profile of photosynthate concentration depends on the initial stem taper and on the conditions at limits (carbon provided by the foliage and carbon given to the roots). As for general carbon allocation patterns (see Warren-Wilson in [42]), stem growth results from a balance between a carbon source (foliage) and the forces of the carbon sinks (the roots and the stem). In our model, the force of the stem sink is driven by the initial stem profile.

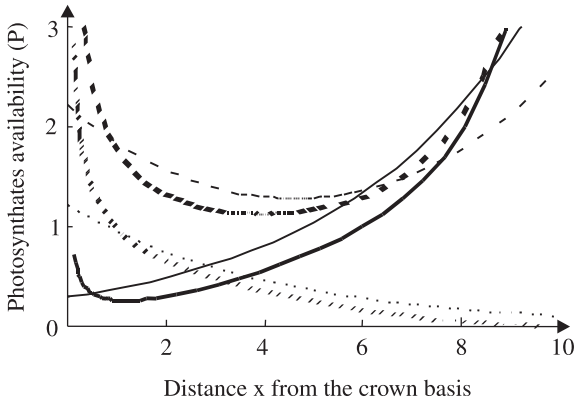

Figure 1. *x*-axis: distance along the stem, measured downward from crown basis. *y*-axis: stem photosynthates concentration. Simulation of photosynthates concentration profiles between crown basis ($x = 0$) and roots ($x = H_c$) with the [Sh] and [Ch] models. Thick lines: the initial shape of the stem is conical; thin lines the initial shape of the stem is cylindrical. Continuous lines: case of a steep profile; broken line: case of a stable profile; points: case of a declining profile.

This general formulation allows for the simulation of the taper of the profile of stem photosynthates concentration, thus the profile of stem radial increment, between crown and roots for different initial conditions (see *figure 1*). The profiles are qualitatively similar for both a conical and a cylindrical stem: the only qualitative is that solutions with a conical stem (combination of Bessel functions) exhibit a sharp increase in photosynthates concentration near $x = 0$ (i.e. just below crown basis).

The models are flexible enough to simulate steeply increasing profiles such as those observed for open-grown trees, thin profiles of suppressed trees, or almost constant profiles of Pressler's rule. Buttress could be generated by these equations with an increase of carbon concentration near the roots. However, the system also predicts a higher consumption of carbon when the initial radius of the stem is larger. Buttress could then be simply described by the initial slow height growth at the juvenile stage of the tree, and an amplification, over the years, of this initial conical shape.

4. CONSTRUCTION OF FLEXIBLE TAPER EQUATIONS FOR RADIAL INCREMENT

From these theoretical solutions we heuristically derive simple functions which aim at describing the vertical variation of stem area increment along the whole

stem. Because exponential profiles for concentration (Eqs. (5–7)) are graphically similar and simpler than the profiles associated to Bessel functions, we combine the concentration profile of a cylindrical stem (Eq. (5)) with the radius increment profile of a conical stem.

Two limit conditions are considered: (i) either foliage and root photosynthates concentrations (P_f and P_r) are fixed; (ii) or carbon flows from foliage (F_f) and to the roots (F_r) are fixed. After noting $z = \sqrt{a'r}$, these conditions become:

$$\text{(i)} \begin{cases} P(x=0) = P_f = A + B \\ P(x=H_c) = P_r = A\exp(-zH_c) + B\exp(zH_c) \end{cases} \quad (12a)$$

$$\text{with} \begin{cases} A = \dfrac{-P_r + P_f \exp(zH_c)}{\exp(zH_c) - \exp(-zH_c)} \\ B = \dfrac{P_r - P_f \exp(-zH_c)}{\exp(zH_c) - \exp(-zH_c)} \end{cases} \quad (12b)$$

$$\text{(ii)} \begin{cases} \dfrac{\partial P}{\partial x}(x=0) = F_f = -zA' + zB' \\ \dfrac{\partial P}{\partial x}(x=H_c) = F_r = -zA'\exp(-zH_c) + zB'\exp(zH_c) \end{cases} \quad (13a)$$

$$\text{with} \begin{cases} A' = \dfrac{F_r - F_f \exp(zH_c)}{z(\exp(zH_c) - \exp(-zH_c))} \\ B' = \dfrac{F_r - F_f \exp(-zH_c)}{z(\exp(zH_c) - \exp(-zH_c))}. \end{cases} \quad (13b)$$

Then:

$$P(x) = \frac{P_r(\exp(zx) - \exp(-zx)) + P_f(\exp(z(H_c - x)) - \exp(-z(H_c - x)))}{\exp(zH_c) - \exp(-zH_c)} \quad (12c)$$

$$P(x) = \frac{F_r(\exp(zx) + \exp(-zx)) - F_f(\exp(z(H_c - x)) + \exp(-z(H_c - x)))}{z(\exp(zH_c) - \exp(-zH_c))}. \quad (13c)$$

Two models of P profiles are derived from equations (12) and (13):

$$P(x) = \frac{P_r \sinh(zx) + P_f \sinh(z(H_c - x))}{\sinh(zH_c)} \quad (12d)$$

$$P(x) = \frac{F_r \cosh(zx) - F_f \cosh(z(H_c - x))}{z\sinh(zH_c)}. \quad (13d)$$

Parameters P_f or F_f control the shape of the curve near the crown, whereas P_r or F_r control its shape near the roots.

The system was initially built for the portion of the stem situated between crown and roots. We will now assume that these profiles can be valid all along the stem, i.e. we replace H_c by the total height H. Under this assumption, the initial stem radius profile is supposed to be a linear function of x: $R(x,0) = \varepsilon x$ ($R(0,0) = R_0 = 0$, at tree tip). The profile of stem area increment ($\Delta G(x)$) is thus obtained by simply multiplying $P(x)$ by εx. Since parameters P_i or F_i and ε are confounded, we simply use P_i and F_i in the rest of the paper. We finally obtain two models, noted: [Sh] and [Ch].

$$[\text{Sh}] \quad \Delta G(x) = x\frac{P_r \sinh(zx) + P_f \sinh(z(H-x))}{\sinh(zH)} \quad (14)$$

$$[\text{Ch}] \quad \Delta G(x) = x\frac{F_r \cosh(zx) - F_f \cosh(z(H-x))}{z\sinh(zH)}. \quad (15)$$

In the previous analysis, a mass loading of carbon is assumed at $x = 0$ (apex). In order to take the distribution of foliage within the crown into account, we propose four other models:

(i): [ShX] and [ChX] with a linear increment of the carbon profile only in the upper part of the stem (F_f and P_f are multiplied by x):

$$[\text{ShX}] \quad \Delta G(x) = x\frac{P_r \sinh(zx) + xP_f \sinh(z(H-x))}{\sinh(zH)} \quad (16)$$

$$[\text{ChX}] \quad \Delta G(x) = x\frac{F_r \cosh(zx) - xF_f \cosh(z(H-x))}{z\sinh(zH)}. \quad (17)$$

(ii): [ShX2] and [ChX2] with a linear increment along the whole stem ($P(x)$ is globally multiplied by x).

$$[\text{ShX2}] \quad \Delta G(x) = x^2\frac{P_r \sinh(zx) + P_f \sinh(z(H-x))}{\sinh(zH)} \quad (18)$$

$$[\text{ChX2}] \quad \Delta G(x) = x^2\frac{F_r \cosh(zx) - F_f \cosh(z(H-x))}{z\sinh(zH)}. \quad (19)$$

In these models, the parameters P_f, F_f, P_r and F_r do not have a biological meaning, but they respectively control the upper part of the stem (inside and near the crown) and the bottom part of the stem (near the roots). Finally we have 4 different models, because [Sh] (resp. [ShX2]) is a reparametrization of the model [Ch] (resp. [ChX2]).

5. MODEL FITTING AND SELECTION

5.1. Model fitting

The 4 models were fitted on data from the 5 stands. Because the parameter z was quite stable, it was first adjusted locally for each curve, and then set to 0.3 for all

Table II. Results of fitting of the 6 models (Eqs. 15–20) on the 5 stands data (Amance or Moncel-sur-Seille). *SSE* is the sum of squared errors (mm^4), *N* is the number of adjusted parameters (number of curves × number of adjusted parameters per curve). Fitting was carried out with the software "Multilisa" developed by Jean-Christophe Hervé (ENGREF, Nancy).

Model	Fitting choice		Stands				
			EEC-s1	**EEC-s2**	**EEC-s3**	**EEC-s4**	**Amance-s5**
Curves number			*186*	*177*	*227*	*228*	*72*
Number of experimental points			*1596*	*1493*	*1934*	*2027*	*1029*
[Sh] or [Ch]	*z* fitted by curve	*SSE*	4.19×10^{-7}	3.77×10^{-7}	5.80×10^{-7}	4.06×10^{-7}	6.92×10^{-8}
		N	558	531	681	684	216
	z set to 0.3	*SSE*	9.60×10^{-8}	8.55×10^{-8}	8.64×10^{-8}	7.16×10^{-8}	1.15×10^{-9}
		N	372	354	454	456	144
[ShX]	*z* fitted by curve	*SSE*	$\mathbf{2.54 \times 10^{-7}}$	$\mathbf{2.61 \times 10^{-7}}$	2.88×10^{-7}	2.24×10^{-7}	5.91×10^{-8}
		N	558	531	681	684	216
	z set to 0.3	*SSE*	$\mathbf{3.22 \times 10^{-8}}$	$\mathbf{2.62 \times 10^{-8}}$	$\mathbf{2.33 \times 10^{-8}}$	$\mathbf{1.80 \times 10^{-8}}$	$\mathbf{6.43 \times 10^{-8}}$
		N	372	354	454	456	144
[ChX]	*z* fitted by curve	*SSE*	7.43×10^{-7}	7.21×10^{-7}	4.58×10^{-7}	5.29×10^{-7}	9.32×10^{-10}
		N	558	531	681	684	216
	z set to 0.3	*SSE*	4.48×10^{-8}	2.73×10^{-8}	2.45×10^{-8}	1.91×10^{-8}	6.59×10^{-8}
		N	372	354	454	456	144
[ShX2] or [ChX2]	*z* fitted by curve	*SSE*	2.72×10^{-7}	2.84×10^{-7}	$\mathbf{2.64 \times 10^{-7}}$	$\mathbf{2.13 \times 10^{-7}}$	$\mathbf{5.69 \times 10^{-8}}$
		N	558	531	681	684	216
	z set to 0.3	*SSE*	3.74×10^{-8}	2.97×10^{-8}	2.83×10^{-8}	2.16×10^{-8}	6.66×10^{-9}
		N	372	354	454	456	144

curves. The value of *H* was set to the observed total height of the tree. The models were fitted with a nonlinear procedure. Results are presented in *table II*. Generally, the [ShX] model gives the best results based on SSE. Convergence of the fitting algorithm is also more efficient for this model (more rapid and not sensitive to the starting values).

Therefore, subsequent analysis focuses on the [ShX] model (Eq. (16)), which has only 3 parameters: P_f and P_r, which are related to foliage and roots vigor, and *z* which is a combination of *r* and *a'*. This model is an empirical function heuristically derived from a process-based analysis of carbon allocation. It is very flexible and can describe profiles coming from suppressed as well as dominant or open-grown trees.

5.2. Sensitivity analysis and biological interpretation of the [ShX] model

Sensitivity analysis of the [ShX] model (Eq. [16]) was performed (*figure 2).* The sensitivity functions exhibit

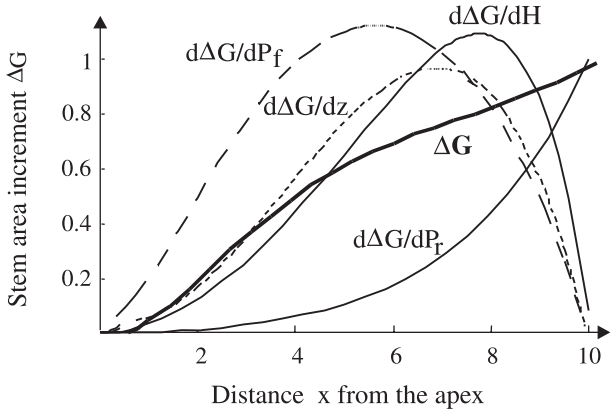

Figure 2. *x*-axis: distance *x* from tree apex. *y*-axis: stem area increment Δ*G* or sensitivity functions. For each sensitivity function, *y*-axis is scaled so that the maximum value is approximately equal to 1: only relative variations are important (derivatives are divided by 10 for Δ*G*, by –0.25 for *H*, by –40 for *z*, by 10 for P_r and by 5 for P_f). Sensitivity analysis of the [ShX] model. Thick line: model [ShX] from $x = 0$ (stem tip) to $x = H$ (soil level). Other lines: sensitivity functions (that is derivatives of [ShX] with respect to each parameter). Parameters are: $H = 10$, $z = 0.3$, $P_r = 1$, $P_f = 1$.

different behaviors, but for $\frac{\partial \Delta G(x)}{\partial H}$ and $\frac{\partial \Delta G(x)}{\partial z}$ which are quite similar. However, H is not a parameter, but a data, so that this similarity does not pose any problem in the nonlinear fitting algorithm. The fact that the fitting algorithm is more efficient for [ShX] model may indeed be explained by the absence of a strong correlation among the sensitivity functions of the three parameters. In order to precisely estimate each parameter, it is theoretically necessary to have data near the point where its derivative peaks: for P_f, data in the upper part of the crown are needed; for P_r, near the bottom of the stem; for z, in the middle of the stem.

Figure 3 shows the effect of each parameter. z controls the flexibility of the profile. In fact, z is a combination of two parameters r and a'; according to [7], a drought would increase r and a fertilization would increase a'. These variations of r and a' result in a thinner increment profile in the bottom. These kind of profiles are observed for suppressed trees. P_f controls the conicity and the upper part of the stem, while P_r controls the butt log. The model [ShX] automatically generates an inflexion point in the upper of the stem, which is rarely described by other models of stem profiles [6].

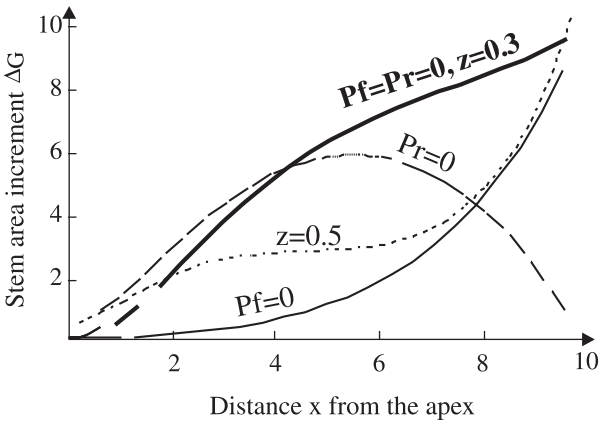

Figure 3. x-axis: distance x from tree apex (m). y-axis: stem area increment ΔG (cm^2 yr^{-1}). Influence of model parameters on the [ShX] model for the profile of stem area increment. Thick line: predicted stem area increment for model ShX with $H = 10$, $z = 0.3$, $P_r = 1$, $P_f = 1$. Other curves: predicted stem area increment for variations around this model: $z = 0.5$, $P_r = 0$, $P_f = 0$.

5.3. Examples of fitted curves

For each site, examples of adjustment are presented: the site of Amance was used to test the flexibility of the model because the measurements were dense along the stem; whereas the 4 stands of Moncel/Seille were used to analyse parameter variability in relation with calendar year, silvicultural treatment and fertility.

5.3.1. Amance site

The trees are young and each annual stem growth unit was sampled. The data are thus very dense along the stem. Adjustment (*figure 4*) is worse for the buttress of the open-grown tree "a1". However, the model [ShX] is quite flexible: it can be fitted to contrasted profiles such as those of "a134" to the more conical form of "a2". The inflexion point near the apex is well described. The other inflexion point near the butt log is less well described.

The parameter z is relatively stable around $z = 0.3$. The shape of the profiles is quite constant. P_f gives the conicity of the profile and depends on tree vigor (high values for steep profiles and small values for declining profiles). P_r is high for all trees at the beginning of growth and decreases after, but for "a1": this decrease

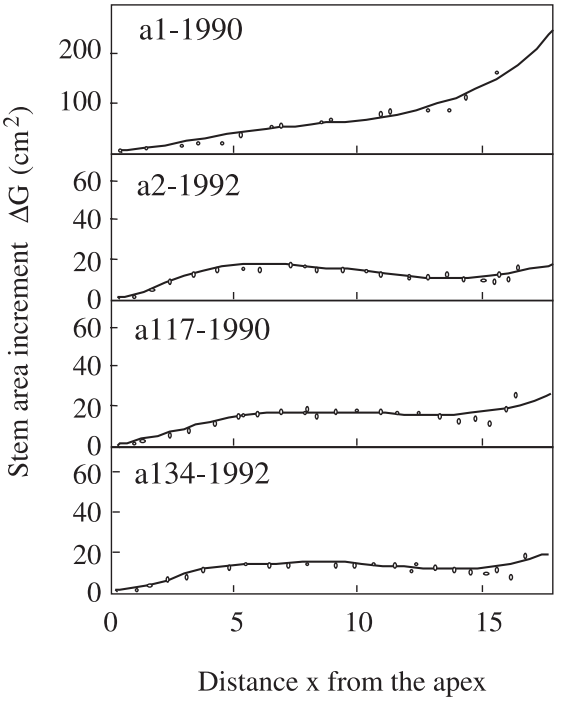

Figure 4. [ShX] model fitted to 4 trees from Amance site. x-axis: distance x from tree apex (m). y-axis: stem area increment ΔG (cm^2 yr^{-1}).

occurs quicker for “a134” than for “a117” and “a2”; which could be a consequence of stand closure that depends on local stand density. Regarding interannual variability, P_r and P_f vary in the same way for all trees *(figure 5)*: this should reflect the role of the annual climatic conditions.

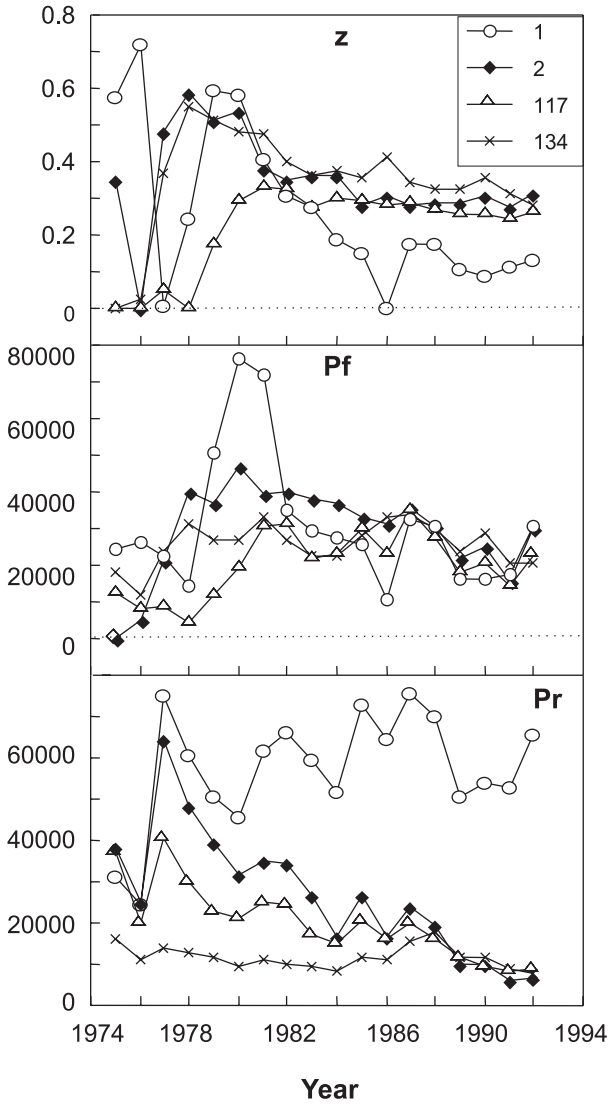

Figure 5. Time evolution of the estimated value of the parameters of [ShX] model, fitted to 4 trees from Amance site. *x*-axis: year of profile formation. *y*-axis: parameters (P_r: cm; P_f: unitless; z: m^{-1}).

5.3.2. Moncel/Seille site

With traditional stem analysis data, the model fits well the shape of the stem increment (*figure 6*). Parameter z does not vary a lot from a stand to another *(figure 7)*. P_f is higher for fertile stands (“s1” and “s2”), resulting in thicker profiles in the upper part of the tree. P_r depends on both site quality and silviculture: good fertility decreases P_r (“s1” and “s2”), whereas thinning increases P_r (“s1” and “s3”).

These results are consistent with classical results: thinning or sparse stands provide steeper profiles [24, 36, 37, 41], whereas site quality increases total production along the whole stem [18, 23, 25, 27, 37, 41]. According to the theoretical model, a larger value of P_r in low site quality stands also reflects a larger share for roots in carbon partitioning.

6. INTEGRATION OF THE TAPER FUNCTION FOR VOLUME PRODUCTION

Predicting or partitioning volume increment are often key objectives of models of radial increment profiles. Some papers have indeed shown the importance of the flexibility of the taper function for the volume estimates [19, 22–24, 29, 33–35]. The model [ShX] has therefore two advantages: it is flexible and it can be analytically integrated. Annual stem volume increment is computed as:

$$\Delta V = \int_{x=0}^{H} \mathrm{d}x \, \frac{P_r \sinh(zx) + xP_f \sinh(z(H-x))}{\sinh(zH)} \qquad (20)$$

$$\Delta V = \frac{Z^2 H P_r \cosh(zH) - Z P_r \sinh(zH) + 2P_f \cosh(zH) - P_f(Z^2 H^2 + z)}{Z^3 \sinh(zH)}.$$

7. DERIVATION OF THE MODEL TO PROVIDE CROWN LIMITS

The variation of the slope along the stem increment profile is usually related to the position of crown base. For example, this assumption has been used to estimate the position of the base of the functional part of the crown from stem analysis data fitted to the Pressler rule [6]. Model [ShX] can be viewed as a generalization of Pressler rule; this model can therefore be used to estimate various singular points along the stem, which can then be linked to crown structure and functioning.

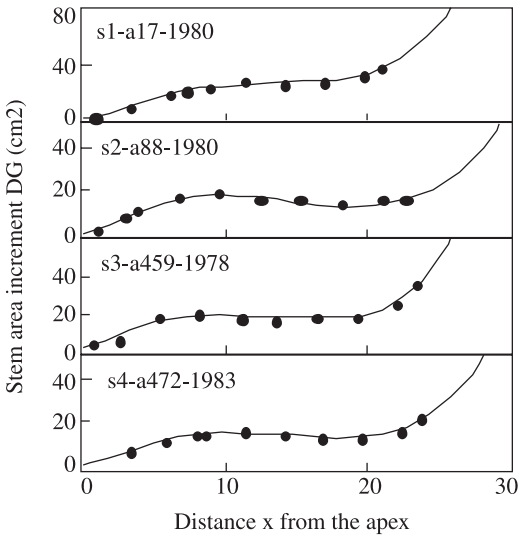

Figure 6. [ShX] model fitted to 4 trees from Moncel/Seille site. *x*-axis: distance *x* from tree apex (m). *y*-axis: stem area increment ΔG (cm^2 yr^{-1}).

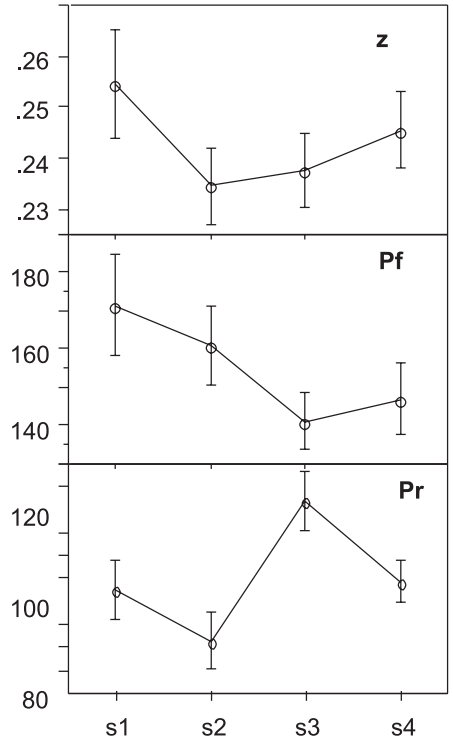

Figure 7. Comparison of the estimated value of the parameters of [ShX] model, fitted to 24 trees from Moncel/Seille site. *x*-axis: stand. *y*-axis: parameters, with their average and 95%-confidence interval (P_r: cm; P_f: unitless; z: m^{-1}).

On the sample trees, we calculated 3 points (H_b, H_f and H_s; see *figure 8*) and compared them with usual crown measurements (H_{fb}, H_{fw} and H_{fc}). H_b is the point, either where stem radial increment is maximum, i.e. $\partial \mathrm{ShX}(x)/\partial x = 0$ (case of a declining profile), or where

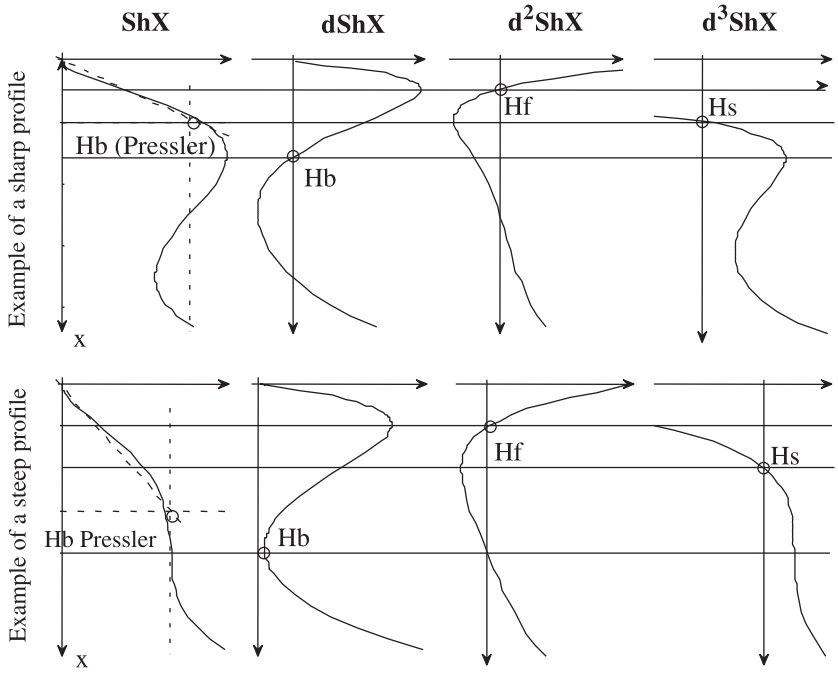

Figure 8. Illustration of how crown basis can be defined from the variation of stem area increment predicted by the [ShX] model. Pressler's crown basis, as defined by Deleuze and Houllier [6], is positioned with broken lines. Top: case of a stressed tree with a sinusoidal increment profile. Bottom: case of a dominant tree with an increasing profile. *y*-axis: distance *x* from the apex. *x*-axis from left to right: predicted stem area increment from the [Shx] model, and its first-, second- and third-order derivatives.

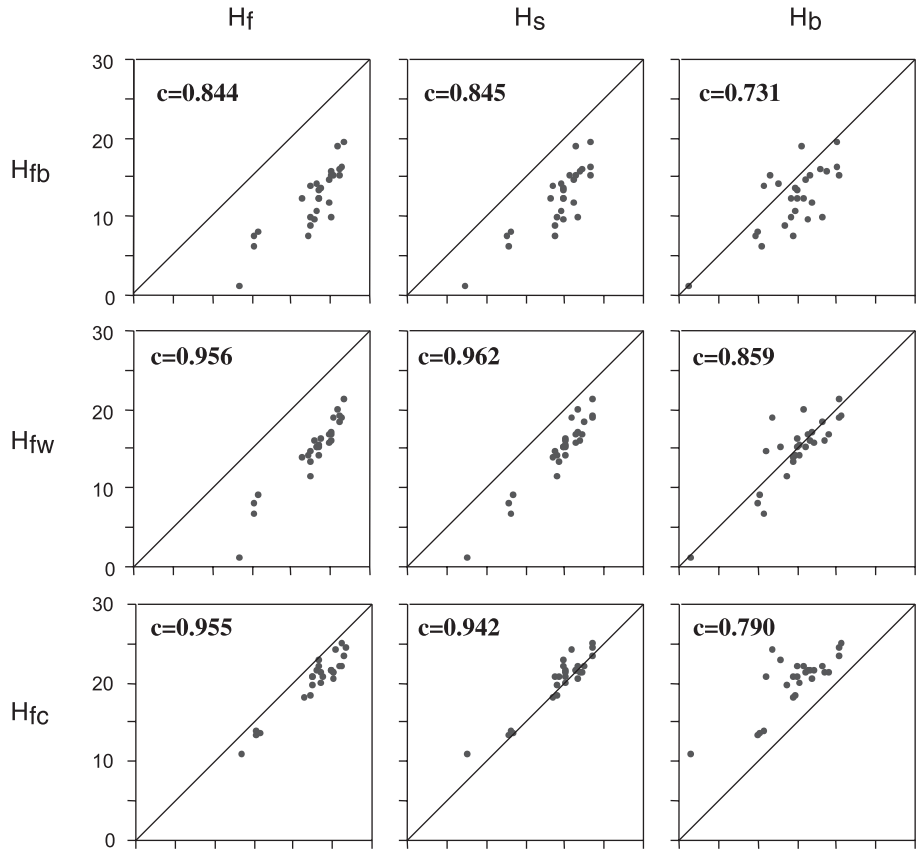

Figure 9. Correlations between theoretical crown basis (H_b, H_f and H_s), derived from the [ShX] model and measured crown basis (H_{fb} first living branch, H_{fw} first living whorl and H_{fc} first contact). All trees are featured. The first bisector line is drawn for each relation.

$\partial \mathrm{ShX}(x)/\partial x$ is minimal (case of a steep profile). H_f is the inflexion point of the profile in the upper part of the stem, i.e. where $\partial^2 \mathrm{ShX}(x)/\partial x^2 = 0$. H_s is an intermediate point where the curvature changes, i.e. where $\partial^3 \mathrm{ShX}(x)/\partial x^3 = 0$. The position of crown basis was also estimated using the Pressler rule criterion [6].

Figure 9 shows the correlation between these theoretical heights and the measured heights. H_{fb} gives the lowest correlations, but this level is quite variable in the crown and highly dependent on local light conditions of the lowest living branches, which do not contribute a lot, if at all, to stem growth. H_{fw} gives the higher correlations and is well connected to H_s. H_{fc} is better related to H_f (inflexion point).

The [ShX] model could thus provide a means to better understand the relationship between external measurements or observations and the internal growth of the stem. This is a key point for growth simulators of tree growth and wood quality, which need to better describe the connection between external environmental conditions of the tree (through the crown structure) and internal stem radial increment and wood formation.

From stem analysis data, we can also reconstruct the past evolution of crown basis. In *figure 10*, two examples are given: the "a17" tree from stand "s1", for which sampling intensity was low and which exhibits an irregular evolution of estimated crown basis H_b; the "a117" tree from stand "s5", for which stem analysis data were more numerous and whose estimated crown recession is more regular. Beside sampling intensity, crown recession of tree "a17" was strongly influenced by the thinning that occurred in 1983, whereas "a117" had a more stable environment (crown recession was more regular and started probably around 1981 when the stand closed).

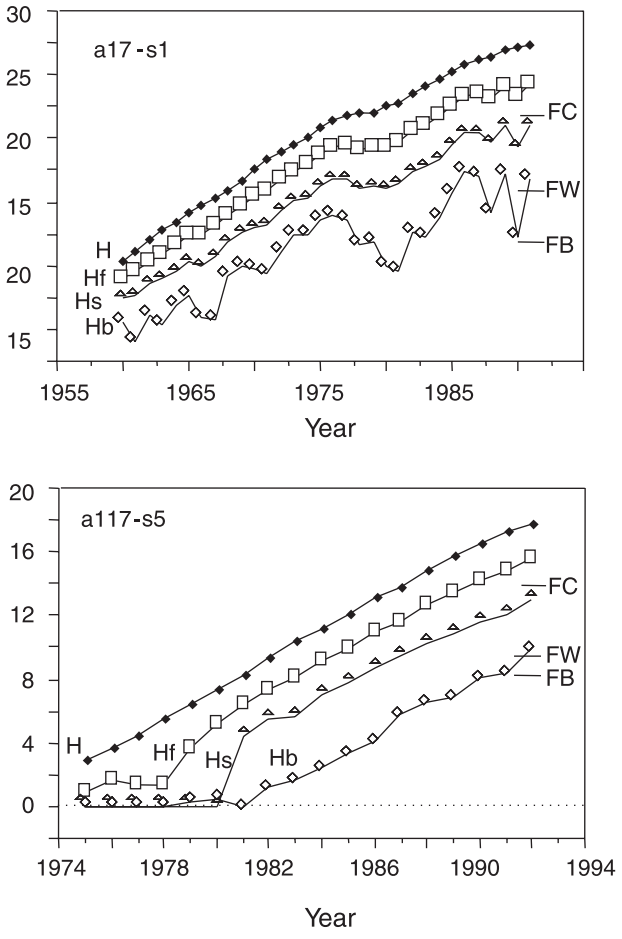

Figure 10. Reconstructed crown recession as predicted from stem analysis data fitted to [ShX] model. *x*-axis: year of growth. *y*-axis: total height H, and heights of theoretical crown basis H_s, H_f and H_b. Measured crown basis are noted for the year of sampling (H_{fc}, H_{fw} and H_{fb}). Top: tree a17 from stand 1 in Moncel/Seille. Bottom: tree a117 from Amance.

8. CONCLUSION

The first result of this study is theoretical: we propose a formal link between carbon partitioning in process-based models and stem radial increment profiles in usual tree growth and yield models. Stem increment profiles are indeed very similar to allocation in the tree. These profiles should therefore be as variable as allocation coefficients, they also should be affected by environmental conditions. The description of cambium as a continuous sink allows to better take secondary growth into account than with a compartment-based tree growth model. The reaction-diffusion model provides a practical tool for describing carbon partitioning among tree compartments and along the stem. The topology and geometry of the tree are thus of prime importance for the carbon distribution. Stem can no more be considered as the third compartment in a standard plant process-based model: the continuous reaction-diffusion model provides a means to account for secondary growth, which is a characteristic feature of the trees.

The second result of this study is practical: we propose a simple parametric equation for modeling the vertical profile of stem radial increment. This model is flexible and accounts for the inflexion point in the upper part of the profiles. It has only 3 parameters that can be interpreted in terms of tree vigor and structure, and that can be related to environmental variations: P_f and P_r are related to total wood production, whereas the ratio P_f:P_r is linked to stem:root carbon partitioning; z seems to be quite stable and independent from external conditions, but it could be variable with species. These parameters are thus synthetic indicators of how trees react to variations in their growth condition.

The third result is a method for reconstructing past crown recession using stem analysis data. This method is based on the analytical study of the shape of the successive radial increment profiles. Stem analysis data contain a lot of information, which could be useful to interpret past growth. We need more data with well known stands to go on with this idea.

Our flexible model is finally a useful tool to extract information from stem analysis or to predict stem growth variations and wood quality from environmental variations. This model should now be applied to other conifers and tested on broadleaves.

Acknowledgments: The authors thank Pr. Anne-Marie Catesson and Dr. Jean-Louis Durand, who provided physiological remarks on the hypothesis, and Dr. Alain Franc for his help in the mathematical analysis. We are also grateful to Dr. Annikki Mäkelä for her comments on the initial manuscript and two anonymous reviewers for their final corrections.

APPENDIX 1: Non stationary solutions of the reaction-diffusion model for an initial cylindrical stem

Equation (4) can be solved using spectral analysis and Fourier transformation (FT) of P. Let $(p,q) \in \mathbf{C}^2$:

$$\mathrm{FT}(P)(p,q) = \frac{1}{2\pi}\int_{\mathrm{R}^2} P(x,t)\exp(-\mathrm{i}px - \mathrm{i}qt)\,\mathrm{d}x\,\mathrm{d}t. \qquad (21)$$

The Fourier transformation of the partial derivatives of P can be simply calculated through an integration by parts. For t:

$$\mathrm{FT}(\frac{\partial P}{\partial t})(p,q)=\frac{1}{2\pi}\int_{\mathrm{R}^2}\frac{\partial P}{\partial t}(x,t)\exp(-\mathrm{i}px-\mathrm{i}qt)\mathrm{d}x\,\mathrm{d}t$$

$$\mathrm{FT}(\frac{\partial P}{\partial t})=\frac{1}{2\pi}\left\{\int_{\mathrm{R}^2}\mathrm{d}x[P(x,t)\exp(-\mathrm{i}px-\mathrm{i}qt)]_{t=-\infty}^{t=+\infty}-\mathrm{i}q\int_{\mathrm{R}^2}\frac{\partial P}{\partial t}(x,t)\exp(-\mathrm{i}px-\mathrm{i}qt)\mathrm{d}x\,\mathrm{d}t\right\} \quad (22)$$

$$\mathrm{FT}(\frac{\partial P}{\partial t})=\mathrm{i}q\mathrm{FT}(P).$$

Similarly, for x we get:

$$\mathrm{FT}(\frac{\partial P}{\partial x})=\mathrm{i}p\mathrm{FT}(P). \quad (23)$$

Equation (4) thus becomes:

$$(\mathrm{i}q+\frac{p^2}{r}+\mathrm{a}')\mathrm{FT}(P)=0. \quad (24)$$

Solution of (24) is the Dirac function $\delta(\mathrm{i}q+\frac{p^2}{r}+\mathrm{a}')$. Solution of (4) is then obtained by the inverse Fourier transformation:

$$P(x,t)=P_0\exp(\mathrm{i}qt+\mathrm{i}px),\ \text{with}\ \ \mathrm{i}q+\frac{p^2}{r}+\mathrm{a}'=0 \quad (25)$$

p and q can be written as:

$$\begin{cases} p=\alpha\mathrm{i}+\beta \\ q=\mathrm{i}\left(a'+\dfrac{\beta^2-\alpha^2}{r}\right)-2\dfrac{\alpha\beta}{r}\end{cases} \quad (26)$$

where α and β are two real constants. Solutions thus become:

$$P(x,t)=P_0\exp\left(\mathrm{i}t\left(\mathrm{i}\left(a'+\frac{\beta^2-\alpha^2}{r}\right)-2\frac{\alpha\beta}{r}\right)+\mathrm{i}x(\alpha\mathrm{i}+\beta)\right)$$

$$P(x,t)=P_0\exp\left(-a't-\frac{\beta^2-\alpha^2}{r}t-\alpha x+\mathrm{i}\left(-2\frac{\alpha\beta}{r}t+\beta x\right)\right). \quad (27)$$

Since only real solutions of P can be acceptable, $\alpha=\frac{rx}{2t}$ and the solutions become:

$$P(x,t)=P_0\exp\left(-a't-\frac{\beta^2}{r}t-\frac{rx^2}{4t}\right) \quad (28)$$

where P_0 and β are calculated thanks to initial and limit conditions. Since r, β^2 and a' are positive, P never runs away.

APPENDIX 2: Stationary solutions of the reaction-diffusion model for an initial conical stem

We solve the general system:

$$\begin{cases}\dfrac{\partial P(x,t)}{\partial t}=0 \\ \dfrac{\partial^2 P(x,t)}{r\partial x^2}-a''xP(x,t)=0\end{cases} \quad (29)$$

where $a''=2\pi a\varepsilon/S$. The analytical solutions are combinations of hyperbolic Bessel functions I^+ and I^- (Gradshteyn and Ryzhik, [11]) which are defined by:

$$\mathrm{I}(n,x)=\frac{(x/2)^n}{\Gamma(n+1/2)\Gamma(1/2)}\int_{-1}^{1}(1-t^2)^{n-1/2}\exp(\pm xt)\mathrm{d}t \quad (30)$$

with $\Gamma(n)=\int_0^\infty t^{n-1}\exp(-t)\mathrm{d}t$

$$\begin{cases}\mathrm{I}^+=\mathrm{I}(\frac{1}{3},\frac{2}{3}\sqrt{a''rx^{3/2}}) \\ \mathrm{I}^-=\mathrm{I}(-\frac{1}{3},\frac{2}{3}\sqrt{a''rx^{3/2}}).\end{cases} \quad (31)$$

There are two independent solutions P_1 and P_2:

$$\begin{cases}P_1(x)=\dfrac{1}{3}\sqrt{\sqrt{a''rx}(\mathrm{I}^--\mathrm{I}^+)} \\ P_2(x)=\sqrt{\dfrac{\sqrt{a''rx}}{3}}(\mathrm{I}^--\mathrm{I}^+).\end{cases} \quad (32)$$

REFERENCES

[1] Assmann E., The principles of forest yield study, Pergamon Press, 1970, 506 p.

[2] Bell A.D., Bryan A., Plant form: an illustrated guide to flowering plant morphology, Oxford University Press, Oxford, 1991, 341 p.

[3] Croc E., Dynamique d'un peuplement forestier hétérogène: modèle de réaction-diffusion, modèle de Turing, Rapport d'option, Département de mathématiques appliquées, École Polytechnique, 1994, 34 p.

[4] Décourt N., Utilisation des dispositifs clinaux pour l'étude de la compétition dans les peuplements forestiers, in: Proceedings of the 5th Conference of Ecology, Paris, France, 12–14 March, 1970, INRA Ed., Nancy, 1970, 17 p.

[5] Deleuze C., Hervé J.C., Colin F., Ribeyrolles L., Modelling crown shape of *Picea abies*, Spacing effects, Can. J. For. Res. 26 (1996) 1957–1966.

[6] Deleuze C., Houllier F., Prediction of stem profile of *Picea abies* using a process-based tree growth model, Tree Physiol. 15 (1995) 113–120.

[7] Deleuze C., Houllier F., A transport model for tree ring width, Silva Fenn. 31 (1997) 239–250.

[8] Dreyfus P., Interaction génotype, densité et compétition dans un dispositif clinal d'Epicéas communs, Ann. Sci. For. 47 (1990) 1–16.

[9] Farrar J.L., Longitudinal variation in the thickness of the annual ring, Forestry Chronicle 37 (1961) 323–330.

[10] Gordon A.J., Graham J.D., Changes in Pinus radiata stem form in response to nitrogen and phosphorus fertiliser, New Zealand J. For. Sci. 16 (1986) 41–54.

[11] Gradshteyn I.S., Ryzhik I.M., Tables of integrals, series and products, Academic Press, 1965, 1086 p.

[12] Hara T., A stochastic model and the moment dynamics of the growth and size distribution in plant populations, J. Theor. Biol. 109 (1984) 173–190.

[13] Hara T., A model for mortality in a self-thinning plant population, Ann. Bot. 55 (1985) 667–674.

[14] Hara T., Growth and competition in clonal plants: persistence of shoot populations and species diversity, Folia Geobot. Phytotax. Praha 29 (1994) 181–201.

[15] Hara T., Wyszomirski T., Competitive asymmetry reduces spatial effects on size-structure dynamics in plant population, Ann. Bot. 73 (1994) 285–297.

[16] Houllier F., Modelling ring width distribution in the tree in relation to silvicultural treatment, in: G. Nepveu (Ed.), Silvicultural control and non destructive assessment of timber quality of plantation grown spruces and Douglas fir, Final report of EC-project-Forest program, Task 3, 1993.

[17] Houllier F., Leban J.M., Colin F., Linking growth modelling to timber quality assessment for Norway spruce, For. Ecol. Manage. 74 (1995) 91–102.

[18] Jack S.B., Stone E.L., Swindel B.F., Stem form changes in unthinned slash and loblolly Pine stands following mid-rotation fertilization, South J. Appl. For. 12 (1988) 90–97.

[19] Kozak A., Smith J.H.G., Standards for evaluating taper estimating systems, Forestry Chronicle 69 (1993) 438–444.

[20] Kozlowski T.T., Carbohydrate sources and sinks in woody plants, Bot. Rev. 58 (1992) 107–222.

[21] Lemoine B., Essai de synthèse biomathématique des aspects concurrentiels, écologiques, morphologiques et cycliques de la croissance du Pin maritime dans la pinède des Landes de Gascogne, Œcologia Plantarum 10 (1975) 141–167.

[22] MacTague J.P., Enhanced estimates of total volume with any single upper-stem measurement, For. Ecol. Manage. 48 (1992) 55–67.

[23] Mead D.J., Tamm C.O., Growth and stem form changes in *Picea abies* as affected by stand stand nutrition, Scand. J. For. Res. 3 (1988) 505–513.

[24] Meng C.H., Detection of stem form change after stand treatment, Can. J. For. Res. 11 (1981) 105–111.

[25] Miller H.G., Cooper J.M., Changes in amount and distribution of stem growth in Pole-stage Corsican pine following application of nitrogen fertilizer, Forestry 46 (1973) 157–190.

[26] Mitchell K.J., Dynamics and simulated yield of Douglas fir, For. Sci, Monograph 17 (1975) 1–39.

[27] Mitchell K.J., Kellog R.M., Distribution of area increment over the bole of fertilized Douglas fir, Can. J. For. Res. 2 (1971) 95–97.

[28] Murray J.D., Mathematical biology. Biomathematics Texts 19, Springer Verlag, Berlin, 1993, 767 p.

[29] Newnham R.M., Variable-form taper functions for four Alberta tree species, Can. J. For. Res. 22 (1992) 210–223.

[30] Okubo A., Diffusion and ecological problems: mathematical models. Biomathematics Texts 10, Springer Verlag, Berlin, 1980, 255 p.

[31] Ottorini J.-M., Growth and development of individual Douglas fir for stands applications to simulation in silviculture, Ann. Sci. For. 48 (1991) 651–666.

[32] Schmid-Haas P., Masumy S.A., Niederer M., Schweingruber F.H., Zuwachs- und Kronenanalysen an geschwächten Tannen. Schweiz, Z. Forstwes. 137 (1986) 811–832.

[33] Sterba H., Radial increment along the bole of trees: problems of measurement and interpretation, in: IUFRO Proceedings: Physiological Aspects and Forest Ecology, Wien. Mittl. d. Forst. Bundesver. (1981) 67–74.

[34] Tarp-Johansen M.J., Skovsgaard J.P., Madsen S.F., Johannsen V.K., Skovsgaard I., Compatible stem taper and stem volume functions for oak (*Quercus robur L.* and *Q. petreæ* (Matt) Liebl) in Denmark, Ann. Sci. For. 54 (1997) 577–595.

[35] Thomas C.E., Parresol B.R., Simple, flexible, trigonometric taper equations, Can. J. For. Res. 21 (1991) 1132–1137.

[36] Thomas C.E., Parresol B.R., Lê K.H.N., Biomass and taper for trees in thinned and unthinned longleaf pine plantations, South. J. App. For. 19 (1995) 29–35.

[37] Thomson A.J., Barclay H.J., Effects of thinning and urea fertilization on the distribution of area increment along the boles of Douglas-fir at Shawnigan Lake, British Columbia, Can. J. For. Res. 14 (1984) 879–884.

[38] Thornley J.H.M., Mathematical models in plant physiology: A quantitative approach to problems in plant and crop physiology, Academic Press, 1976, 318 p.

[39] Thornley J.H.M., Johnson I.R., Plant and crop modelling: a mathematical approach to plant and crop physiology, Clarendon press, Oxford, 1990.

[40] Väisänen H., Kellomäki S., Oker-Blom P., Valtonen E., Structural development of Pinus sylvestris stands with varying initial density: a preliminary model for quality of sawn timber as affected by silvicultural measures, Scand. J. For. Res. 4 (1989) 223–238.

[41] Valinger E., Effects of thinning and nitrogen fertilization on stem growth and stem form of *Pinus sylvestris* trees, Scand. J. For. Res. 7 (1992) 219–228.

[42] Wyse R.E., Sinks as determinants of assimilate partitioning possible sites for regulation, in: Cronshaw J., Lucas W.J., Giaquinta R.T. (Eds.): Phloem transport, New York, (1986) 197–209.